

Utilization of Mud Weights in Excess of the Least Principal Stress to Stabilize Wellbores: Theory and Practical Examples

Takatoshi Ito, SPE, Tohoku U.; Mark D. Zoback, SPE, Stanford U.; and Pavel Peska, GeoMechanics Intl.

Summary

In this paper, we address the theoretical possibility of drilling with mud weights in excess of the least principal stress for cases of particularly high pore pressure or severe wellbore instability. Because lost circulation caused by hydraulic fracturing is to be avoided, we consider three critical wellbore pressures, p_{frac} , p_{link} , and p_{grow} . Tensile fractures initiate at the wellbore wall at p_{frac} , link up to form large axial fractures that are subparallel to the wellbore axis at p_{link} , and propagate away from the wellbore at p_{grow} . It is obvious that lost circulation cannot occur if the wellbore pressure during drilling is below p_{frac} . However, even if p_{frac} is exceeded and tensile fractures are initiated at the wellbore wall, fracture propagation (and, hence, lost circulation) will be limited as long as the wellbore pressure is below p_{link} . Finally, if the wellbore pressure is greater than p_{link} , the fractures will not grow away from the wellbore (and significant lost circulation will not occur) if the wellbore pressure is below p_{grow} , which must exceed (if only slightly) the least principal stress. In general, our modeling shows that p_{frac} and p_{link} can be maximized by drilling the wellbore in an optimally stable orientation, and p_{grow} can be maximized with noninvading drilling muds that prevent fluid pressure from reaching the fracture tip. We apply the model that uses in-situ stress data collected in real fields, such as the South Eugene Island field in the Gulf of Mexico and the Visund field in the northern North Sea.

Introduction

In this paper, we theoretically investigate the circumstances under which it may be possible to drill with mud weights in excess of the least principal stress in extreme drilling environments. To accomplish this, we must avoid lost circulation caused by the propagation of hydraulic fractures. We consider the case of an arbitrarily oriented well with a perfect mudcake such that in the absence of hydraulic fracturing, no drilling fluids leave the wellbore. We consider a three-fold strategy to maximize, to the greatest degree possible, mud weights during drilling. To accomplish this, we use the following facts.

- Wellbore pressure at fracture initiation varies with the wellbore deviation and azimuth.¹⁻⁴
- Because deviated wells are generally not parallel to one of the principal stresses, multiple tensile fractures form in an en-echelon pattern on opposite sides of the wellbore wall.⁵ Wellbore pressure and orientation determine whether these multiple fractures link up.⁶
- When drilling with high solids water-based muds, pressures in the wellbore may not reach the fracture tip because of the narrow width of the fracture and the bridging of solids within it.^{7,8}

Taking these facts into account, we develop a theoretical model to estimate the critical pressures that dominate hydraulic fracture initiation and propagation. The pressure necessary to initiate fractures at the wellbore wall is first. Second is what is required to link the inclined tensile fractures near the wellbore wall, and third is what is required to extend the fracture instability away from the wellbore. To the degree to which we can predict these pressures, we can potentially raise mud weights to deal with problems of extreme wellbore instability, especially in cases of extremely high pore pressure, in which the difference between the pore pressure

and the fracture gradient is quite small. We apply the model shown here to the stress state encountered in real fields, such as the Visund and the South Eugene Island fields, and demonstrate how to maximize wellbore pressures during drilling by controlling wellbore orientation and mud parameters.

Fracture Model

Tensile Fracture Initiation. Let us consider the stress state in a plane tangent to an arbitrarily oriented wellbore (Fig. 1). In the plane, the tangential stress s_t is given by

$$s_t = \frac{1}{2}(s_{zz} + s_{\theta\theta}) + \frac{1}{2}(s_{zz} - s_{\theta\theta}) \cos 2\omega + s_{\theta z} \sin 2\omega, \quad \dots \quad (1)$$

where s_t deviates by the angle ω from the wellbore axis, and $s_{\theta\theta}$, s_{zz} , and $s_{\theta z}$ = the stress components at the wellbore wall in a wellbore cylindrical coordinate system (r , θ , z) (see Refs. 9 and 10). Compressive stresses are positive in this paper. Note that $s_{\theta\theta}$, s_{zz} , and $s_{\theta z}$ change with wellbore orientation and the state of remote stresses, but $s_{\theta\theta}$ also changes with wellbore pressure. According to the Terzaghi effective stress law, the effective stress component of s_t is given by

$$\sigma_t = s_t - p_p, \quad \dots \quad (2)$$

where σ_t = the effective stress, and p_p = the formation pore pressure. The minimum value σ_{tmin} is given by

$$\sigma_{tmin} = \frac{1}{2}(s_{zz} + s_{\theta\theta}) - \frac{1}{2} \sqrt{(s_{zz} - s_{\theta\theta})^2 + 4s_{\theta z}^2} - p_p. \quad \dots \quad (3)$$

Note that σ_{tmin} is a function of θ . If σ_{tmin} goes into tension at certain angles of θ , tensile wall fractures will initiate at these points, provided σ_{tmin} overcomes the tensile strength of rock, T_0 .¹⁻⁵ In other words, the tensile fractures will initiate when the following occurs.

$$\sigma_{tmin} = -T_0. \quad \dots \quad (4)$$

T_0 is frequently expected to be very close to zero because some pre-existing flaws or irregularities are usually present on the wellbore wall.¹¹ In this paper, T_0 is assumed to be zero. The wellbore pressure at fracture initiation (i.e., wellbore pressure that satisfies Eq. 4) is hereafter referred to as the initiation pressure and is denoted as p_{frac} .

Every two points on the wellbore wall, identified by θ and $\theta + 180^\circ$, have the same $s_{\theta\theta}$, s_{zz} , and $s_{\theta z}$, but with opposite signs (see Refs. 9 and 10). Eq. 3 shows that the sign of $s_{\theta z}$ does not play a role in the value of σ_{tmin} because $s_{\theta z}$ appears in a quadratic form. This means that if σ_{tmin} satisfies Eq. 4, the fracture initiates normal to σ_{tmin} at $\theta = \theta_f$ and at $\theta = \theta_f + 180^\circ$. The fractures deviate from the wellbore axis by the angle ω_f (see Fig. 2), where

$$\omega_f = \frac{1}{2} \tan^{-1} \left(\frac{2s_{\theta z}}{s_{zz} - s_{\theta\theta}} \right). \quad \dots \quad (5)$$

This equation shows that if the fracture angle at $\theta = \theta_f$ is $\omega = \omega_f$, its angle at $\theta = \theta_f + 180^\circ$ is $\omega = -\omega_f$ because of the difference in the sign of $s_{\theta z}$. As a result, the fractures will appear as en-echelon sets in wellbores, the axis of which inclined to all of the principal stress

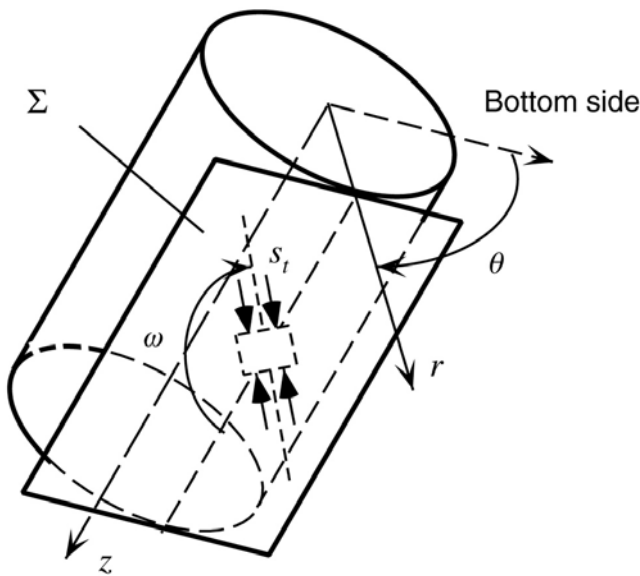


Fig. 1—The coordinate system used in this study and the tangential stress s_t in a plane tangent to the wellbore (plane Σ).

axes. Such fractures have been observed in numerous wellbores,¹²⁻¹⁴ as illustrated in Fig. 2.

Fracture Linkup. As long as the wellbore axis deviates from the principal stress directions, the fractures will initiate at angle ω_f toward the wellbore axis, as shown in Fig. 2. As long as the wellbore pressure is lower than a critical value (discussed later), the fractures will propagate over a relatively narrow range of angles along the wellbore wall and will not link up, owing to nonuniform distribution of σ_t and interference between adjacent fractures.⁶ A small fracture length along the wellbore wall suggests a small fracture opening at the wellbore wall especially compared to the opening of large, axial, hydraulically driven fractures that occur once the small fractures have linked up. Conversely, if the wellbore axis is nearly parallel to one principal stress direction, the fractures will initiate parallel to the wellbore axis and will form a pair of axial fractures on opposite sides of the wellbore. The opening of the fractures is, again, relatively large, and linkup is not a factor. If the fracture is modeled as a so-called Perkins-Kern-Nordgren (PKN) fracture,¹⁵ the fracture opening is proportional to the fracture length along the wellbore wall. Thus, if the length of an inclined fracture and an axial fracture is 0.1 and 10 m, respectively, the opening of the axial fracture is approximately 100 times larger than that of the inclined fracture. If the fracture opening is small, the opening could be sealed with the appropriate drilling muds, and significant circulation loss could be prevented.

Now let us consider the critical pressure, p_{link} , at which inclined tensile fractures at the wellbore wall would be likely to link up to form large axial fractures. In principle, the linkup phenomenon will be dominated by the stress state in plane Σ tangent to the wellbore. We disregard the existence of the fracture toughness of rock here because the compressive stresses acting in plane Σ are so large that their effect on the fracture propagation is expected to be very large compared to the effect of the fracture toughness. The stresses acting parallel and normal to the fracture in plane Σ are denoted as s_{para} and s_{norm} , respectively. Fluid pressure within the fracture is assumed to be the same as the wellbore pressure p_w . In general, the fluid pressure in the fracture must be equal to or larger than s_{norm} for a fracture to grow. The following two cases, 1 and 2, can be considered at the fracture growing.

- Case 1 $p_w = s_{norm}, > s_{para}$.
- Case 2 $p_w > s_{norm}, s_{para} > s_{norm}$.

In this study, s_{para} and s_{norm} are taken to be approximated by

$$s_{para} = s_t |_{\omega=\omega_f} \dots \dots \dots (6)$$

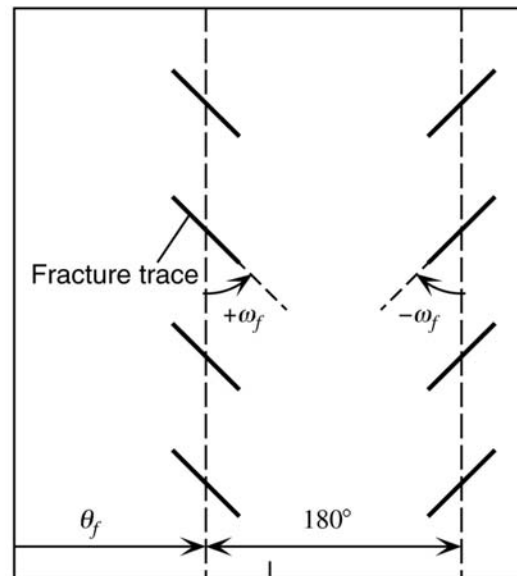


Fig. 2—Unwrapped image of an arbitrarily oriented wellbore with drilling-induced tensile wall fractures (after Brudy and Zoback⁶).

$$\text{and } s_{norm} = s_t |_{\omega=\omega_f+90^\circ} \dots \dots \dots (7)$$

Note that s_{para} and s_{norm} will change with p_w , in contrast to ω_f , which is given by p_{frac} .

Case 1. When p_w reaches s_{norm} , the fractures will start to grow. The fractures will grow by reorienting themselves to normal to s_{para} values in this case because they tend to grow normal to the minimum compressive stress. As a result, the fractures will grow toward adjacent fractures and will finally link up to form the axial fractures. Therefore, the critical wellbore pressure at the linkup, p_{link} , can be estimated by solving the equation $p_w = s_{norm}$.

Case 2. Under a stress state that leads to $s_{para} \geq s_{norm}$, the fracture will always grow in a direction parallel to the initial fracture. However, because there is interference between adjacent fractures, the fractures will reorient themselves to deviate from the direction of the initial fracture line, but only under a certain combination of s_{para} , s_{norm} , and p_w . Weng⁶ carried out a 2D analysis of the linkup problem of en-echelon fractures, taking into account the interference between them, and obtained a criterion that defines the linkup phenomenon. Although his analysis was originally conducted for the case of fractures that link up in a region away from a wellbore, we adopt this criterion here to approximate fracture linkup near the wellbore wall. The criterion is expressed as

$$\omega_f \leq \omega_{crit} \dots \dots \dots (8)$$

$$\text{where } \omega_{crit} = \sin^{-1} \left[0.57 \left(\frac{\Delta s}{\Delta p} \right)^{-0.72} \right] \dots \dots \dots (9)$$

and

$$\Delta s = s_{para} - s_{norm} \dots \dots \dots (10)$$

$$\Delta p = p_w - s_{norm} \dots \dots \dots (11)$$

The numeric constants in Eq. 9 (i.e., 0.57 and 0.72) were obtained by numerical simulations of fracture linkup.⁶ Fig. 3 shows the critical angle ω_{crit} for fracture linkup calculated from Eq. 9. For inclined fractures with angle ω_f more than the critical angle curve, the fractures will not link up. For inclined fractures with ω_f less than the critical angle curve, the fractures will link up. However, ω_{crit} is a function of p_w . For initial fractures with a given ω_f , the critical wellbore pressure p_{link} at which the initial fractures just link up to form the axial fractures can be estimated by substituting ω_{crit} for ω_f in Eq. 9 and solving for p_w .

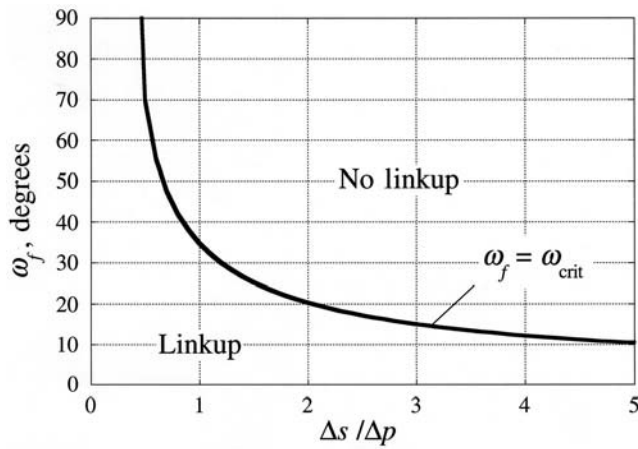


Fig. 3—Critical fracture angle controlling the linkup of inclined fractures near the wellbore to form large axial fractures.

Thus, the procedure to estimate p_{link} is summarized as follows.

- For a given set of remote stresses and wellbore orientations, estimate ω_f with the equations presented in the previous section.
- Estimate the wellbore pressure p_w that will satisfies $p_w = s_{norm}$. Note that s_{norm} is a function of p_w . The estimated p_w is denoted here as p^* .
- If $s_{norm} > s_{para}$ at $p_w = p^*$, then $p_{link} = p^*$.
- If $s_{norm} \leq s_{para}$ at $p_w = p^*$, then p_{link} is estimated by substituting ω_{crit} for ω_f in Eq. 9 and solving for p_w .

Fracture Propagation. Once the inclined tensile fractures link up, the hydraulically driven fractures will tend to propagate away from the wellbore and reorient themselves to be normal to the minimum remote stress s_3 because wellbore-induced stresses diminish quickly away from the wellbore.¹⁶ The experiments carried out by Behrmann and Elbel¹⁷ indicated that this reorientation can take place even within one wellbore diameter under certain stress conditions. Afterward, the fractures will propagate, keeping their surfaces normal to s_3 .¹⁸

Now let us consider the fluid pressure necessary to drive fracture propagation away from a wellbore. To this end, the fracture is assumed to be large compared to the wellbore size and is modeled as a penny-shaped fracture, oriented normal to s_3 . Pressure distribution in the fracture is assumed as shown in Fig. 4, where we take into account the fact that drilling fluids containing solids may prevent pressure from reaching the fracture tip if, because of its narrow width, the solids effectively plug the fracture.^{7,8} For simplicity, we assume that the pressure is uniform at p_{grow} , except for

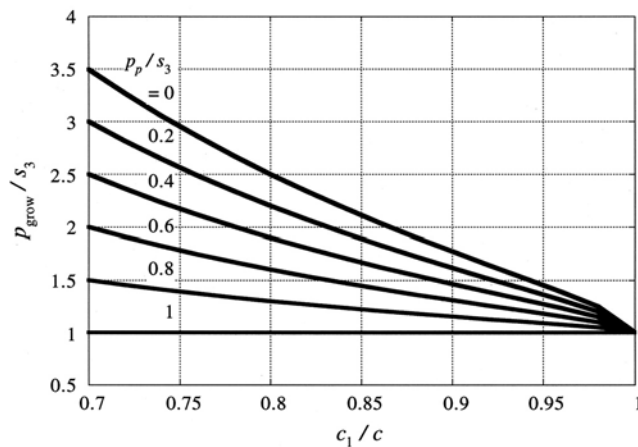


Fig. 5—Variation of the fracture-propagation pressure with the size of the noninvaded zone for different ratios of pore pressure to the least principal stress. Note that this is likely a lower-bound estimate of p_{grow}/s_3 , as a uniform pressure distribution is assumed in the invaded zone.

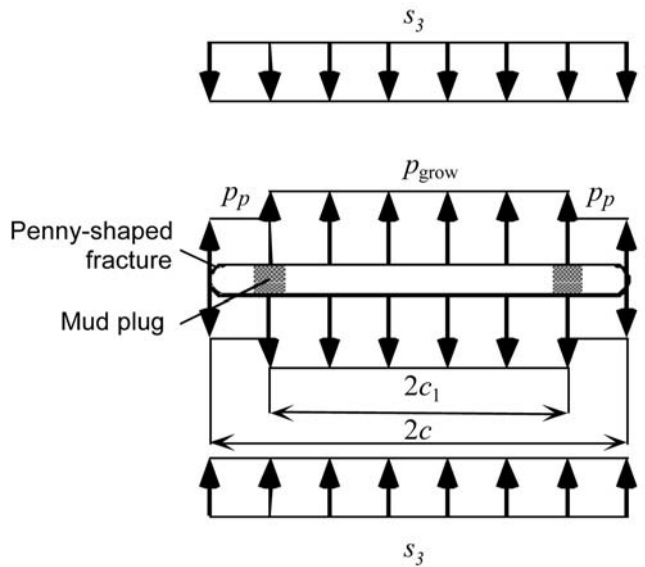


Fig. 4—Definition of the invaded zone ($2c_1$), where the internal pressure is p_{grow} , and the noninvaded zone ($c-c_1$), where the internal pressure during fracture growth is p_p .

a zone at the fracture tip where the drilling fluid does not reach and pressure remains equal to the pore pressure p_p . We refer to these as the invaded and the noninvaded zones, respectively. For this case, Abé *et al.*¹⁹ derived a theoretical relationship between p_{grow} , p_p , and s_3 . The relationship is given by

$$\frac{p_{grow} - s_3}{s_3 - p_p} = \frac{1}{1 - \sqrt{1 - \left(\frac{c_1}{c}\right)^2}} \left[\sqrt{1 - \left(\frac{c_1}{c}\right)^2} + \sqrt{\frac{\pi}{4c} \frac{K_{IC}}{s_3 - p_p}} \right], \quad \dots \dots \dots (12)$$

where K_{IC} = the fracture toughness of the rock, and c and c_1 = the radius of the fracture and that of the invaded zone, respectively. K_{IC} can be neglected for large size fractures, such as the fracture we consider here.²⁰ Therefore, from Eq. 12, we come up with the following equation.

$$\frac{p_{grow}}{s_3} = \frac{1 - \frac{p_p}{s_3} \sqrt{1 - \left(\frac{c_1}{c}\right)^2}}{1 - \sqrt{1 - \left(\frac{c_1}{c}\right)^2}} \quad \dots \dots \dots (13)$$

The relationship between p_{grow}/s_3 and c_1/c , obtained from Eq. 13, is plotted in Fig. 5. This figure shows that the existence of the noninvaded zone contributes to maximize p_{grow} . The p_{grow} is hereafter referred to as the fracture-propagation pressure. Note that Eq. 13 gives a lower limit of p_{grow} . If a pressure gradient exists in the fracture because of fluid flow, p_{grow} will be even larger than that given by Eq. 13 and shown in Fig. 5. The fractures will not grow significantly as long as the wellbore pressure is lower than p_{grow} , even if tensile fractures are initiated at the wellbore. However, if p_p takes exactly the same value as s_3 , the noninvaded zone will not contribute at all to raise p_{grow} in excess of s_3 independent of the size of the noninvaded zone (i.e., c_1/c).

Fuh *et al.*²¹ argue that special loss-prevention material (LPM) can be used to enhance the noninvaded zone and report dramatically increased fracture-propagation pressures; pressures increased by as much as 8 lb/gal in one well and 3 to 6 lb/gal in others. Note that Fuh *et al.*²¹ presented an equation that gives a theoretical relationship between p_{grow} and the fracture width at the inlet of the noninvaded zone (i.e., W_c), which is basically the same as Eq. 12. Laboratory experiments by Morita *et al.*⁸ indicate that p_{grow} is higher with water-based muds because the noninvaded zone was larger than with oil-based muds. Such a difference in the size of the non-

invaded zone with mud types may be caused because a certain degree of filtrate loss from fracture surfaces is required to form the noninvaded zone. For the same reason, the noninvaded zone will not be formed effectively in impermeable rocks.

Case Studies

The analysis previously presented suggests that mud weight during drilling can be maximized in two ways without loss of circulation. First, because both the initiation pressure p_{frac} and the linking pressure p_{link} depend on wellbore orientation, p_{frac} and p_{link} can potentially be maximized by drilling in an optimal direction. Second, because drilling with a noninvading mud will inhibit fluid pressure from reaching the fracture tip (i.e., $c_1/c \leq 1$), p_{grow}/s_3 will increase, as illustrated in Fig. 5.

The following example illustrates a practical application of these concepts to a lost circulation episode in a well drilled in the Gulf of Mexico. Lost circulation occurred at an equivalent circulating density (ECD) of 14.8 lb/gal during a surge that occurred inadvertently while attempting to free a stuck logging tool. The measured value of the least principal stress at this depth was 13.0 lb/gal. To regain circulation, lost circulation material (LCM) was used, and circulation was established at 14.9 lb/gal, which is 1.9 lb/gal in excess of the least principal stress and 0.1 lb/gal in excess of the pressure at which circulation was initially lost. Because a fracture had already propagated from the wellbore, we can evaluate the influence of the LCM that prevented pressure propagation to the tip of the fracture (Fig. 5). For appropriate values of stress, pore pressure, well deviation, etc., the theoretical p_{grow} would be 15.0 lb/gal (consistent with the observation of recovering circula-

tion at 14.8 lb/gal), assuming that $c_1/c=0.95$. As noted below, this value of c_1/c is quite reasonable because values found in laboratory experiments and other studies^{8,21,24} imply that c_1/c can even attain lower values. Moreover, once circulation was re-established, drilling ahead was accomplished at ECDs equivalent to 13.6 to 14.4 lb/gal, again in excess of the least principal stress. This is a straightforward explanation of the theoretical fracture-initiation and linkup pressures.

Another practical example for a deviated well being planned for the Caspian Sea is shown in Fig. 6. In this case, the well plan uses the wellbore collapse pressure as the lower bound for the safe-drilling mud window. When the least principal stress was used as the upper bound of the mud window, four strings of casing were required. (see Fig. 6, left). However, taking into account that there cannot be lost circulation if there is no fracture linkup, using the linkup pressure as the upper bound for the mud window allows the well to be drilled with one fewer casing strings (see Fig. 6, right). While the p_{link} is appreciably greater than the least principal stress over a considerable range of depths, the fact that p_{link} was greater by approximately 0.2 specific gravity (SG) at ~4350 m meant that it would be possible to run the 11.75-in. casing to the total depth (TD).

We can apply the analysis presented in this paper more generally with the in-situ stress data obtained in the Visund field (Block 34/8) of the northern North Sea and the South Eugene Island field (Blocks 316 and 338) offshore Louisiana in the Gulf of Mexico. The stress states and pore pressures in the fields are listed in Table 1, where S_{Hmax} , S_{Hmin} , and S_V are the maximum and minimum horizontal stresses and the vertical stress, respectively, from Finkbeiner and Zoback²² and Wiprut and Zoback.²³ The least principal stresses

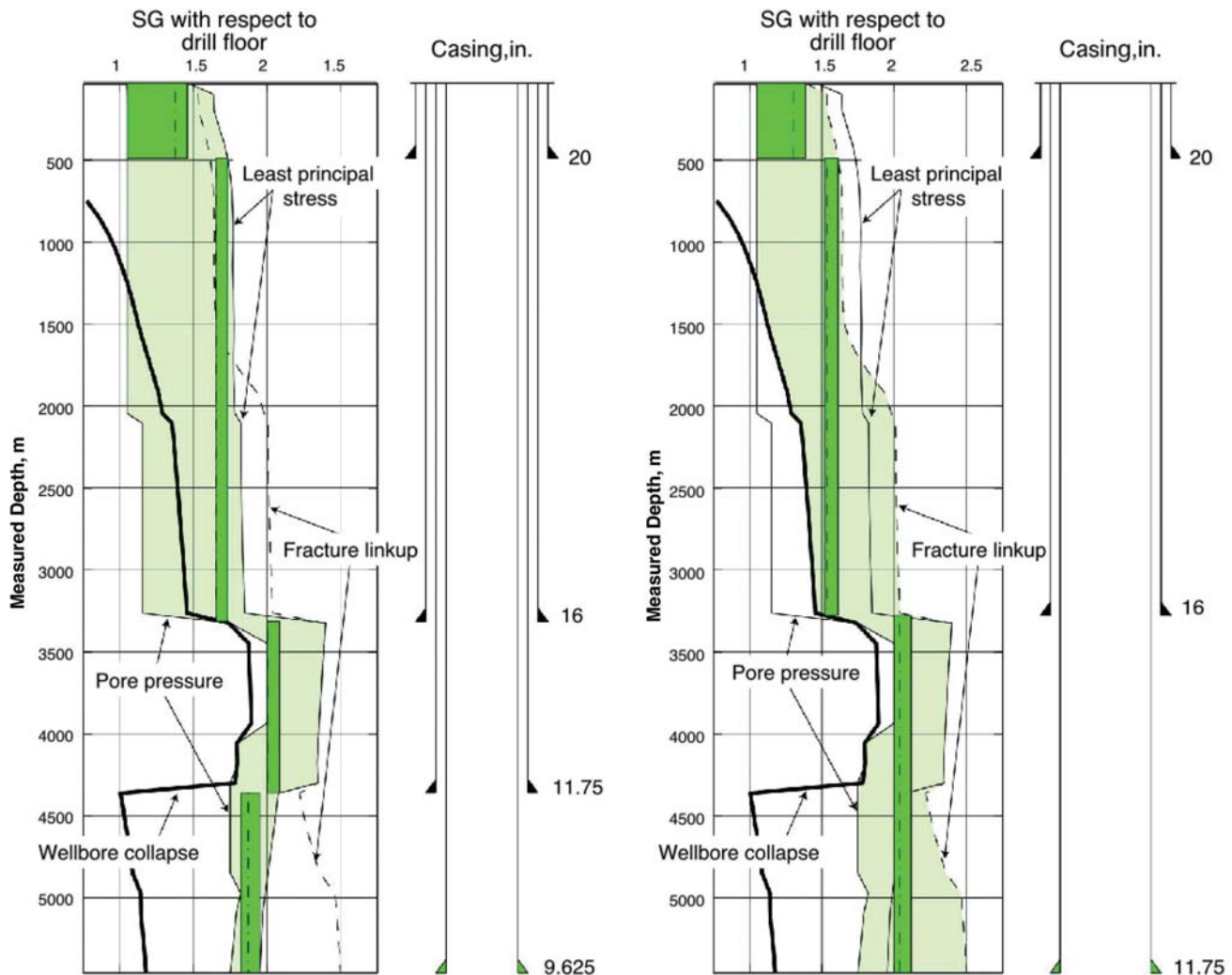


Fig. 6—Mud windows and casing plans for a well planned in the Caspian Sea. In both panels, the lower bound of the safe-drilling window is the wellbore collapse pressure. The two cases shown consider the least principal stress as the upper bound of the safe drilling window (left) and p_{link} (right). With p_{link} , we achieve an increase in the mud window sufficient to save one casing string.

TABLE 1—STRESSES AND PORE PRESSURE VALUES USED FOR EXAMPLES IN FIGS. 7 THROUGH 10

Well	Depth	s_v	s_{Hmin}	s_{Hmax}	p_p	η	λ	Azimuth of s_{Hmax}	C_0^*	p_{grow}^{**}	
										$c_1/c = 1$	0.85
Visund 10S	9,285 ft	7,990 psi	7,712 psi	10,367 psi	6,380 psi	0.26	0.80	N97E	2,900 psi	7,712 psi	9,195 psi
		16.56 lb/gal	15.98 lb/gal	21.48 lb/gal	13.22 lb/gal	15.98 lb/gal	19.05 lb/gal				
SEI 338/A8	6,814 ft	6,267 psi	5,415 psi	6,130 psi	4,698 psi	0.14	0.75	N140E	2,800 psi	5,415 psi	6,213 psi
		17.70 lb/gal	15.29 lb/gal	17.31 lb/gal	13.27 lb/gal	15.29 lb/gal	17.54 lb/gal				
SEI 316/A12	6,985 ft	6,335 psi	6,300 psi	6,315 psi	6,137 psi	0.01	0.97	N100E	350 psi	6,300 psi	6,481 psi
		17.45 lb/gal	17.35 lb/gal	17.39 lb/gal	16.90 lb/gal	17.35 lb/gal	17.85 lb/gal				
Modified A8	6,814 ft	6,267 psi	5,415 psi	6,130 psi	5,311 psi	0.14	0.85	N140E	2,800 psi	5,415 psi	5,530 psi
		17.70 lb/gal	15.29 lb/gal	17.31 lb/gal	15.00 lb/gal	15.29 lb/gal	15.62 lb/gal				

*Compressive strength of rock

**Values are for water-based mud, assuming an invaded zone along 85% of the length of the hydraulic fracture propagating from the wellbore (i.e., $c_1/c = 0.85$). For oil-based mud, we assume that $c_1 = c$ and $p_{grow} = s_{Hmin}$.

were measured by the leakoff tests in the Visund field and by the minifracure tests in the South Eugene Island field within an accuracy to $\pm 3\%$. The data listed as Modified A8 in Table 1 are assumed. The Visund field is in a strike-slip faulting stress regime, and the South Eugene Island field is in a normal-faulting stress regime. All the wells considered are overpressured; only the South Eugene Island Well 316/A12 is severely overpressured. In Table 1, η and λ = nondimensional parameters that are defined as follows.

$$\eta = \frac{s_1 - s_3}{s_1}, \dots \dots \dots (14)$$

and $\lambda = \frac{p_p}{s_v}, \dots \dots \dots (15)$

where s_1 = the maximum principal stress. η and λ are introduced to classify the degree of the stress anisotropy and the overpressured state of a well, respectively. They take values of between zero and one, respectively (i.e., $0 \leq \eta \leq 1, 0 \leq \lambda \leq 1$). With a larger η , the stress state is more anisotropic. With a larger λ , the well is more overpressured.

When drilling with a fully invading mud, we assume that $c_1/c = 1$ (i.e., fluid pressure in a propagating hydraulic fracture reaches the tip of the fracture with essentially no diminution of pore pressure) to investigate the influence of the type of mud used during drilling. In this case, p_{grow} is simply equal to the least principal stress, s_{Hmin} , in the three cases simulated here. However, in the case of a noninvading mud, the values for p_{grow} , shown in Table 1, assume that $c_1/c = 0.85$. The value of 0.85 yields fracture-propagation pressures that are generally consistent with the field²¹ and laboratory tests^{8,24} mentioned previously as well as empirical drilling experience that higher mud weights can be attained with water-based muds, which tend to be more noninvading. For the Visund 10S well, an 85% invading mud will yield an increment in mud weight of ~ 3 lb/gal (see Table 1), which is, perhaps, analogous to the cases cited by Fuh *et al.*²¹

In Figs. 7 through 9, we demonstrate the relative stability of wells of different orientations at the depths of interest. In each figure, the azimuth of a well corresponds to the angular position around the plot, and the deviation corresponds to the radial distance from the center of the plot.⁴ In such figures, the relative stability of wells of different orientations can be easily compared. The color in each figure defines the mud-weight value required to inhibit failure, as defined later.

In Fig. 7, we consider the Visund 10S well, which is characterized by an anisotropic, strike-slip stress field ($\eta = 0.25$) and modest overpressure ($\lambda = 0.8$). Fig. 7a illustrates the excess mud weight required to prevent breakouts from occurring that span more than 80° of the wellbore circumference. In other words, the calculated mud weights allow limited failure of the wellbore wall but not severe failure. We refer to this pressure as p_{bo} . Note that to prevent excessive wellbore failure, a mud weight of ~ 15 lb/gal is generally required, even though wells that are highly deviated to the west/northwest (or east/southeast) are more stable and can be drilled with a lower mud weight.²³ As pointed out by Wiprut and Zoback,²³ these calculations are in accordance with the drilling experience of 10 wells in the Visund field. The next question is:

how high of a mud pressure could one use without potential loss of circulation? Fig. 7b illustrates that the formation of tensile fractures at the wellbore wall are quite likely if mud weights of close to 15 lb/gal are used. Thus, if one uses a sufficiently high mud weight to prevent breakouts, with the exception of wells that are highly deviated in an approximately east/west direction, it is likely that drilling-induced tensile fractures will be present. While this is, once again, consistent with drilling experience in this field,²³ the formation of cracks in the wellbore wall are not problematic if no lost circulation occurs.²³ Fig. 7d indicates a maximum of p_{frac} , p_{link} , and p_{grow} , where it is assumed that a fully invading mud is used in the well (i.e., assuming $p_{grow} = s_{Hmin} = 15.98$ lb/gal). This figure indicates that one could, in general, use a mud weight of 15.98 lb/gal ($= p_{grow}$) without potential loss of circulation. Thus, in this case, there is an appreciable, safe-drilling mud window of 15 to 16 lb/gal, in which wellbore stability can be maintained, and lost circulation can be prevented, even in the worst case (i.e., that one is drilling with a fully invading mud and the wellbore intersects with pre-existing fractures that are quite large compared to the wellbore diameter). If the pre-existing fractures are small, one could maximize mud weights up to 19.97 lb/gal by directional drilling so as to maximize p_{link} because fractures cannot grow significantly as long as they do not link up near the wellbore.

Fig. 8 shows mud-weight calculations for South Eugene Island Well 338/A8, which is moderately overpressured ($\lambda = 0.75$) and has moderate stress anisotropy ($\eta = 0.14$). In this case, a mud weight of 13.35 to 13.59 lb/gal is required to maintain wellbore stability. Wells deviated in a northeast or southwest direction are slightly more stable than wells of similar deviations at other azimuths. If a fully invading drilling mud is used, unstable fracture propagation occurs at a mud weight essentially equal to the least principal stress. Because this pressure is 1.7 lb/gal more than the pressure required to maintain wellbore stability (see Table 1), an ample safe-drilling mud window (13.59 to 15.29 lb/gal) is available. If needed, one could maximize mud weights sufficiently up to 18.46 lb/gal (see Fig. 8c) by directional drilling so as to maximize p_{link} . Note that p_{frac} is higher for a well than p_{link} . However, pre-existing flaws at the wellbore wall could potentially help fractures initiate. Thus, it is more reasonable to consider the fracture-linkup propagation pressure than the fracture-initiation pressures in such calculations.

Fig. 9 shows a similar analysis for South Eugene Island Well 316/A12, which is severely overpressured ($\lambda = 0.97$) and characterized by very little stress anisotropy ($\eta = 0.01$). In this case, mud weights slightly larger than the pore pressure are sufficient to prevent compressive failure of the wellbores. Thus, the lower bound of the mud windows in this field is controlled by the pore pressure, in contrast to the other two fields, where they are controlled by breakouts. Because of the high overpressure, there is a very small difference between the pore pressure and the least principal stress ($p_p = 16.90$ lb/gal and $s_3 = 17.35$ lb/gal), and the potential for lost circulation during drilling is a serious threat. If a fully invading drilling mud is used, unstable fracture propagation occurs at a mud weight of 17.35 lb/gal (i.e., $p_{grow} = 17.35$ lb/gal). If one uses a non-invading drilling mud and the mud pressure invades a propagating fracture along 85% of its length, a modest gain of the maximum mud weight of ~ 0.5 lb/gal is achievable.

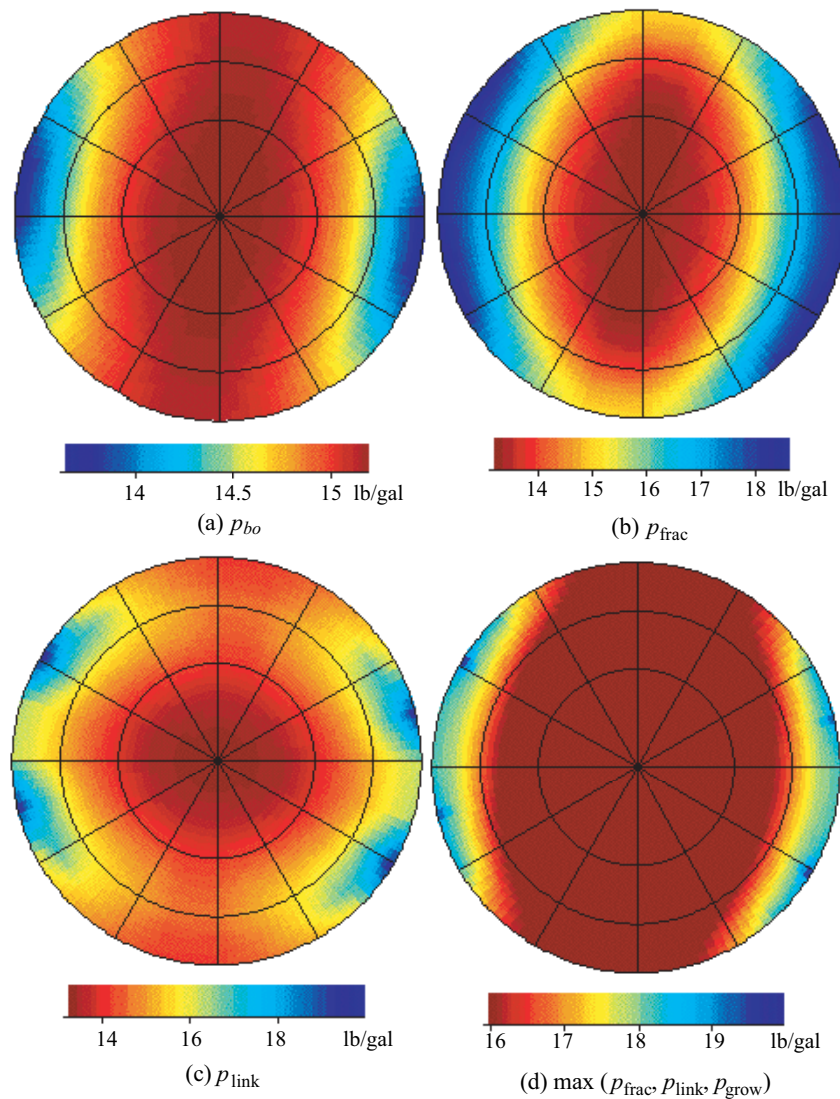


Fig. 7—Mud weights required for wellbore stability as a function of hole azimuth and deviation for the Visund 10S well. (a) Mud weights required to limit compressive failure, p_{bo} . (b) Mud weights to induce tensile failures at the wellbore wall, p_{frac} . (c) Mud weights at which fractures link up near the wellbore, p_{link} . (d) Maximum of p_{frac} , p_{link} , and mud weights at which unstable hydraulic fracture propagation occurs, and p_{grow} , where it is assumed that a fully invading mud is used in the well (i.e., assuming $p_{grow} = s_{hmin}$).

It is easily understood that if the stress state is isotropic, p_{frac} and p_{link} take exactly the same values, respectively, independent of the wellbore orientation. Thus, the dependence of p_{frac} and p_{link} on wellbore orientation are classified by the stress anisotropy parameter η . The larger η is, the more p_{frac} and p_{link} change with wellbore orientation, and they could be maximized efficiently by drilling the wellbore in an optimum orientation. The dependence of p_{frac} and p_{link} on wellbore orientation are affected by not only η but also the parameter λ . p_{frac} decreases with increasing p_p . A smaller p_{frac} (compared with the averaged remote stress) causes fractures to be inclined more steeply relative to the wellbore axis (i.e., fractures with a larger ω_f). The larger ω_f is, the harder it is for the fractures to link up at a low wellbore pressure so that p_{link} increases with ω_f . As a result, p_{link} increases with p_p , but p_{frac} decreases with increasing p_p . For this reason, with a larger λ (i.e., the more overpressured well), p_{link} could be maximized more efficiently by drilling the wellbore in an optimum orientation. For example, if p_p increases from 13.27 to 15 lb/gal ($\sim s_3$), as in the case of South Eugene Island Well 338/A8, p_{link} for the wellbore in an optimum orientation increases from 18.48 lb/gal (Fig. 7c) to 18.90 lb/gal as shown in Fig. 10. Contrary to this, p_{frac} for the wellbore in an optimum orientation decreases from 20.84 lb/gal (Fig. 8b) to 18.07 lb/gal (Fig. 10b). Furthermore, the increase in p_p reduces p_{grow} from 17.54 to 15.62 lb/gal, even though an 85% invading mud is assumed. As noted in the previous section, if p_p is equal to s_3 , p_{grow} will be equal to s_3 , independent of the size of the noninvaded zone. Furthermore,

the noninvaded zone will not be formed effectively in impermeable rocks. In those cases, directional drilling to maximize p_{link} will be the only potential way to maximize mud weights in excess of s_3 . Because fluid-loss additives may help inhibit fracture linkup, they have the potential advantage of stopping fracture propagation at the wellbore as well as increasing fracture-propagation pressures.

Conclusions

The analysis presented here illustrates the theoretical pressures at which inadvertent hydraulic-fracture initiation and propagation might occur during drilling. Because drilling with mud weights of greater than the least principal stress may sometimes be necessary, the analysis presented here can provide insight into how to accomplish this. The application of the theory presented here demonstrates that mud weight during drilling can be maximized without loss of circulation in two ways. First, because both the fracture-initiation pressure, p_{frac} , and the fracture-linking pressure, p_{link} , depend on wellbore orientation, even in the presence of pre-existing fractures at the wellbore wall, p_{link} can potentially be maximized by drilling in an optimal direction. Second, because drilling with a noninvading mud will inhibit fluid pressure from reaching the fracture tip, this will increase the fracture propagation pressure p_{grow} , as noted by previous works.^{8,21} However, this method for maximizing p_{grow} is limited in wells that are severely overpressured. In such a case, attempting to maximize p_{link} with directional drilling can be especially important.

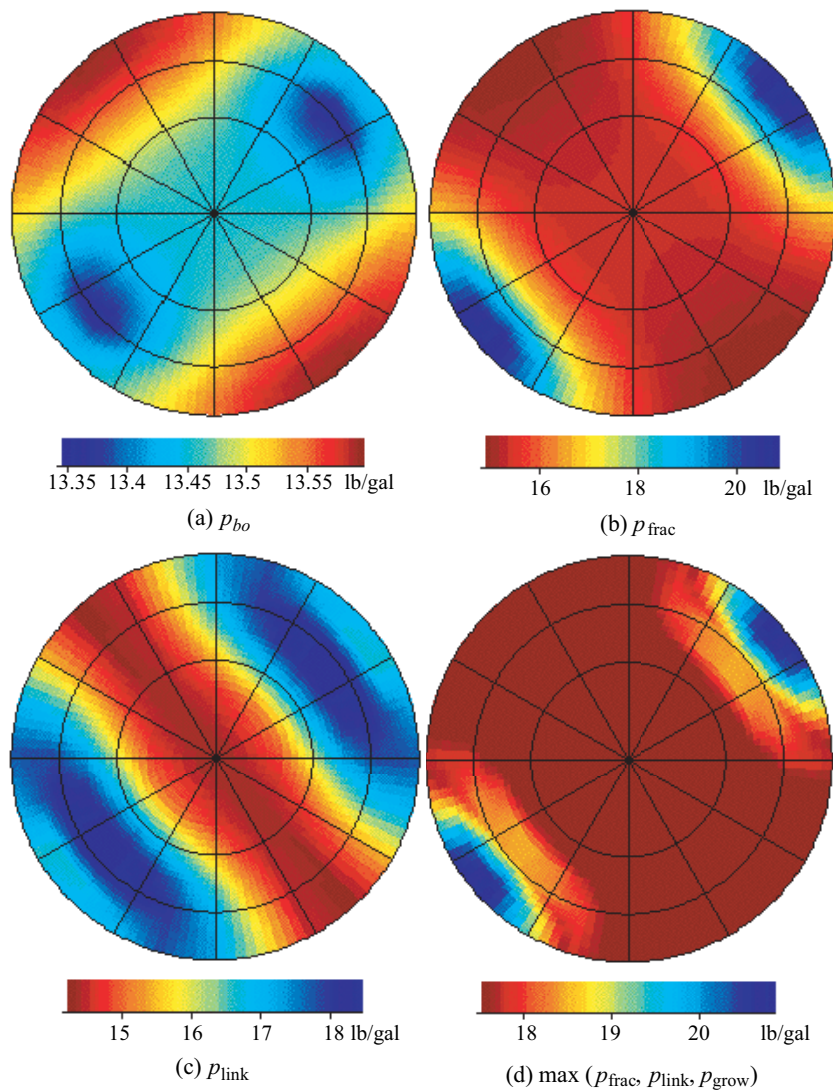


Fig. 8—Mud weights required for wellbore stability as a function of hole azimuth and deviation for the South Eugene Island Well 338/A8, where an 85% invading mud is assumed to estimate p_{grow} .

Nomenclature

c = radius of fracture, L, m
 c_1 = radius of invaded zone in fracture, L, m
 K_{IC} = fracture toughness of rock, $m/L^{1/2} t^2$, $kPa \cdot m^{1/2}$
 p_{bo} = pressure required to limit compressive failure at wellbore wall, m/Lt^2 , kPa
 p_{frac} = fracture-initiation pressure, m/Lt^2 , kPa
 p_{grow} = fracture-propagation pressure, m/Lt^2 , kPa
 p_{link} = critical pressure to link inclined fractures at wellbore wall, m/Lt^2 , kPa
 p_p = formation pore pressure, m/Lt^2 , kPa
 p_w = fluid pressure in wellbore, m/Lt^2 , kPa
 r, θ, z = cylindrical coordinates
 s_1 = greatest principal stress, m/Lt^2 , kPa
 s_3 = least principal stress, m/Lt^2 , kPa
 s_{hmin} = least horizontal principal stress, m/Lt^2 , kPa
 s_{Hmax} = greatest horizontal principal stress, m/Lt^2 , kPa
 s_{norm} = stress normal to initial fractures in a plane tangent to wellbore, m/Lt^2 , kPa
 s_{para} = stress parallel to initial fractures in a plane tangent to wellbore, m/Lt^2 , kPa
 s_t = tangential stress at wellbore wall, m/Lt^2 , kPa
 s_v = vertical stress, m/Lt^2 , kPa
 $s_{\theta\theta}, s_{zz}, s_{\theta z}$ = stress components in a plane tangent to wellbore, m/Lt^2 , kPa

T_0 = tensile strength of rock, m/Lt^2 , kPa
 W_c = fracture width at an inlet of noninvaded zone, L, m
 $\Delta p = p_w - s_{norm}$, m/Lt^2 , kPa
 $\Delta s = s_{para} - s_{norm}$, m/Lt^2 , kPa
 η = stress anisotropy parameter
 θ_f = fracture orientation in θ
 λ = ratio of formation pore pressure to overburden
 σ_t = effective stress component of s_t , m/Lt^2 , kPa
 $\sigma_{t \min}$ = least value of s_t , m/Lt^2 , kPa
 ω = angle relative to wellbore in a plane tangent to wellbore
 ω_{crit} = critical fracture-inclination angle
 ω_f = fracture-inclination angle

Acknowledgments

Financial support for this work was provided by Stanford Rock Physics and the Borehole Geophysics Consortium. We thank Eric van Oort for stimulating us to address this problem.

References

1. Daneshy, A.A.: "A Study of Inclined Hydraulic Fractures," *SPEJ* (April 1973) 61.
2. Hayashi, K. *et al.*: "A New In-Situ Tectonic Stress Measurements and Its Application to a Geothermal Model Field," *Geothermal Resources Council Trans.* (1985) 9, 99.

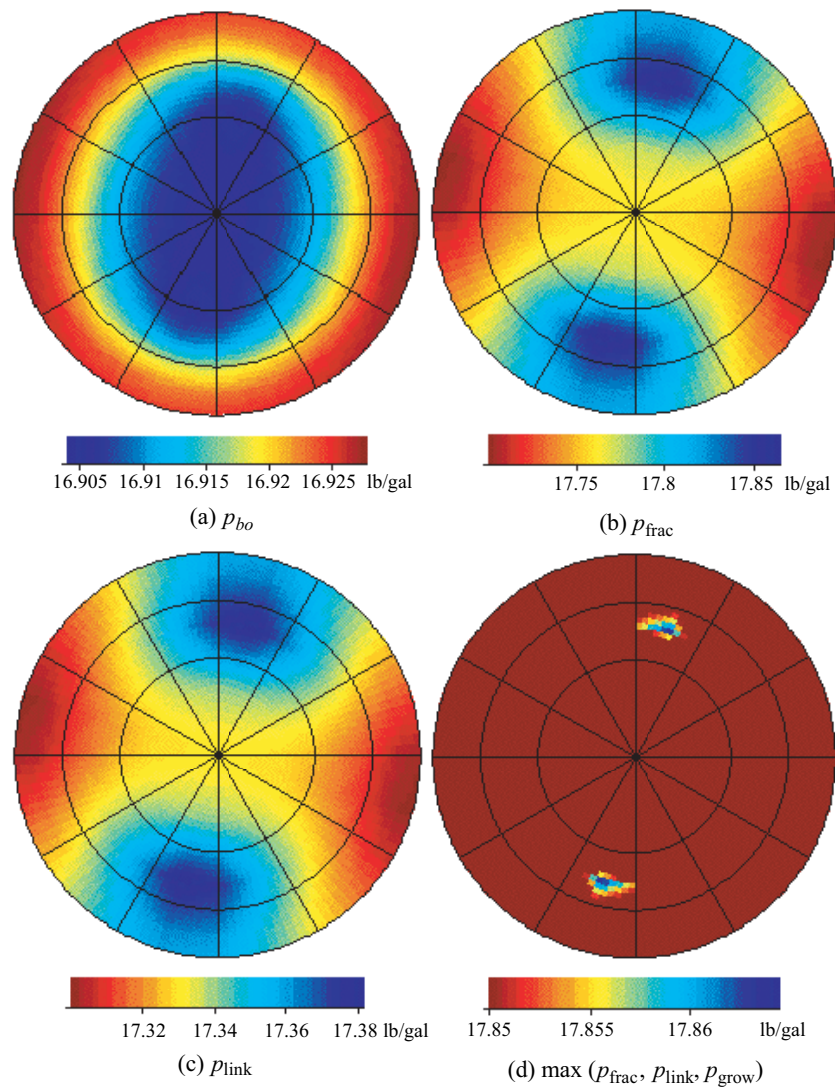


Fig. 9—Mud weights required for wellbore stability as a function of hole azimuth and deviation for the South Eugene Island 316/A12 well, where an 85% invading mud is assumed to estimate p_{grow} .

3. Hayashi, K., Sato, A., and Ito, T.: "In-Situ Stress Measurements by Hydraulic Fracturing for a Rock Mass with Many Planes of Weakness," *Intl. J. Rock Mech. and Min. Sci.* (1997) **34**, No. 1, 45.
4. Peska, P. and Zoback, M.D.: "Compressive and Tensile Failure of Inclined Wellbores and Determination of In-Situ Stress and Rock Strength," *J. Geophys. Res.* (1995) **100**, No. B7, 12791.
5. Brudy, M. and Zoback, M.D.: "Compressive and Tensile Failure of Boreholes Arbitrarily Inclined to Principal Stress Axes: Application to the KTB Boreholes, Germany," *Intl. J. Rock Mech. and Min. Sci.* (1993) **30**, No. 7, 1035.
6. Weng, X.: "Fracture Initiation and Propagation From Deviated Wellbores," paper SPE 26597 presented at the 1993 SPE Annual Technical Conference and Exhibition, Houston, 3–6 October.
7. Black, A.D.: "Investigation of Lost Circulation Problems with Oil Base Drilling Fluids," *DRL Repts: Phase I* (1986).
8. Morita, N., Black, A.D., and Fuh, G.F.: "Borehole Breakdown Pressure with Drilling Fluids—I. Empirical Results," *Intl. J. Rock Mech. and Min. Sci.* (1996) **33**, No. 1, 39.
9. Hiramatsu, Y. and Oka, Y.: "Stress Around a Shaft or Level Excavated in Ground with a Three-Dimensional Stress State," *Mem. Fac. Eng. Kyoto U.* (1962) V.XXIV, Part 1, 56.
10. Fairhurst, C.: "Methods of Determining In-Situ Rock Stresses at Great Depths," technical report, TRI-68, Missouri River Div. Corps of Engineers, Omaha, Nebraska (1968).
11. Bradley, W.B.: "Failure of Inclined Boreholes," *J. Energy Res. Tech., Trans. ASME* (1979) **102**, No. 4, 232.
12. Brudy, M. and Zoback, M.D.: "Drilling-Induced Tensile Wall Fractures: Implications for Determination of In-Situ Stress Orientation and Magnitude," *Intl. J. Rock Mech. and Min. Sci.* (1999) **36**, No. 2, 191.
13. Kuriyagawa, M. *et al.*: "Application of Hydraulic Fracturing to Three-Dimensional In-Situ Stress Measurement," *Intl. J. Rock Mech. and Min. Sci.* (1989) **26**, No. 6, 587.
14. Okabe, T., Shinohara, N., and Takasugi, S.: "Earth's Crust Stress Field Estimation by Using Vertical Fractures Caused by Borehole Drilling," paper presented at the 1996 Intl. Symposium Observation of the Continental Crust Through Drilling, Tsukuba, Ibaraki, 26–28 February.
15. Nordgren, R.P.: "Propagation of a Vertical Hydraulic Fracture," *SPEJ* (August 1972) 306.
16. Kirsch, G.: "Die Theorie der Elastizität und die Bedürfnisse des Festigkeitslehre," *VDI Z* (1898) **42**, 707.
17. Behrmann, L.A. and Elbel, J.L.: "Effect of Perforations on Fracture Initiation," paper SPE 20661 presented at the 1992 SPE Annual Technical Conference and Exhibition, New Orleans, 23–26 September.
18. Hubbert, M.K. and Willis, D.G.: "Mechanics of Hydraulic Fracturing," *Trans. AIME* (1957) **210**, 153.
19. Abé, H., Mura, T., and Keer, L.M.: "Growth Rate of a Penny-Shaped Crack in Hydraulic Fracture of Rocks," *J. Geophys. Res.* (1976) **81**, No. 29, 5335.
20. Barenblatt, G.I.: "The Mathematical Theory of Equilibrium Cracks in Brittle Materials," *Advances in Applied Mechanics*, H.L. Dryden and T. von Karman (eds.), Academic Press, New York (1962) **7**, 55.
21. Fuh, G.F. *et al.*: "A New Approach to Preventing Lost Circulation While Drilling," paper SPE 24599 presented at the 1992 SPE Annual Technical Conference and Exhibition, Washington, D.C., 4–7 October.
22. Finkbeiner, T. and Zoback, M.D.: "Characterization of the Full Stress Tensor in Eugene Island Block 330, Offshore Gulf of Mexico,"

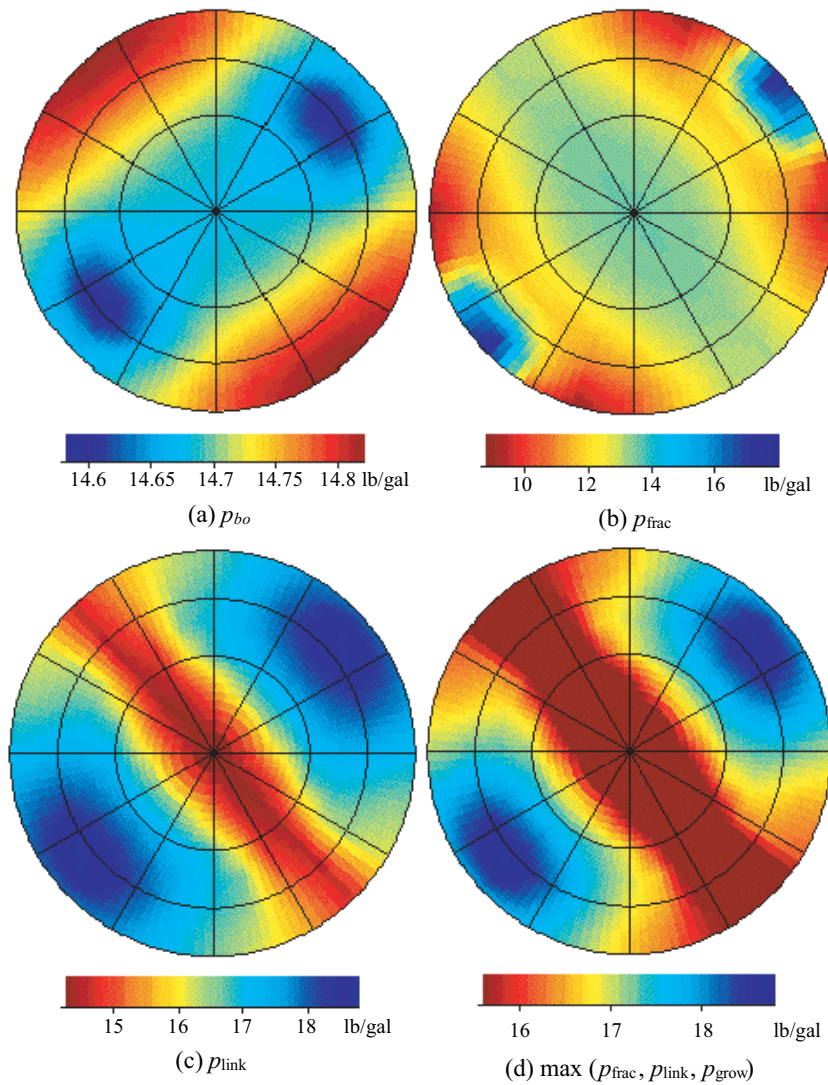


Fig. 10—Mud weights required for wellbore stability as a function of hole azimuth and deviation for a model case, where an 85% invading mud is assumed to estimate p_{grow} . The assuming data are basically the same as the data for the South Eugene Island 338/A8 well except for pore pressure. In this case, the assumed pore pressure is closer to the least principal stress than the pore pressure for the South Eugene Island 382/A8 well (see Table 1).

Stanford Rock Physics & Borehole Geophysics Project Annual Report, Stanford, California (June 1998) F6.

23. Wiprut, D. and Zoback, M.D.: "Constraining the Full Stress Tensor in the Visund Field, Norwegian North Sea," Stanford Rock Physics & Borehole Geophysics Project Annual Report, Stanford, California (June 1998) F2.
24. Willson, S.M. *et al.*: "Laboratory Investigation of Drill Cuttings Disposal by Downhole Injection," paper presented at the 1999 U.S. Rock Mech. Symp., Vail, Colorado, 6–9 June.

SI Metric Conversion Factors

ft × 3.048*	E – 01 = m
psi × 6.894 757	E – 00 = kPa
gal × 3.785 412	E – 03 = m ³
lbm × 4.535 924	E – 01 = kg

*Conversion factor is exact.

SPEDC

Takatoshi Ito is currently an associate professor of rock mechanics at the Inst. of Fluid Science, Tohoku U. e-mail: ito@ifs.tohoku.ac.jp. He was previously employed at Stanford U. as a visiting associate professor to work with the Group for Stanford Rock Physics and Borehole Geophysics Project. Ito holds a degree in mechanical engineering from Tohoku U. **Mark D. Zoback** is currently a professor of geophysics at Stanford U. e-mail: zoback@pangea.stanford.edu. Previously, he was a geophysicist at the USGS, serving as Chief of the Branch of Tectonophysics. In 1996, he cofounded GeoMechanics Intl., a consulting and software firm serving the petroleum industry. Zoback holds a PhD in geophysics from Stanford U. **Pavel Peska** is a senior vice president at GeoMechanics Intl., where he is responsible for software development in areas of in-situ stress and wellbore stability. e-mail: peska@geomi.com. He was previously a visiting scientist at Stanford U. in the Dept. of Geophysics and a department head of the Geophysical Inst., Academy of Sciences, Prague, Czech Republic. Peska holds a PhD in geophysics from Charles U. in Prague.